Natural Products and Bioprospecting

ORIGINAL ARTICLE

Cyclic heptapeptides with metal binding properties isolated from the fungus *Cadophora malorum* from Antarctic soil

Guidmar C. Donalle[1,2†], María Martha Martorell[3†], Gastón E. Siless[1,2], Lucas Ruberto[3*] and Gabriela M. Cabrera[1,2*] (ID)

Abstract

The Antarctic fungus *Cadophora malorum* produces previously undescribed cyclic heptapeptides (cadophorin **A** and **B**) containing an anthranilic acid residue. The planar structure of these peptides was determined by high-resolution mass spectrometry combined with extensive 1D and 2D NMR spectroscopy. The absolute configuration of the amino acids was determined by Marfey's method, with HPLC analysis of FDVA (Nα-(2,4-dinitro-5-fluorphenyl)-L-valinamide) derivatives making use of a PFP column. Remarkably, cadophorin **2** possesses both the uncommon D-Ile and D-*allo*-Ile in its structure. The peptides have metal binding properties as shown by LCMS with *post column* addition of metal salt solutions. These results were supported by DFT calculations.

Keywords: Cyclic peptide, *Cadophora malorum*, Metal binding

†Guidmar C. Donalle and María Martha Martorell contributed equally to this work

*Correspondence: luruberto@gmail.com; gabyc@qo.fcen.uba.ar

[1] Facultad de Ciencias Exactas y Naturales, Departamento de Química Orgánica, Universidad de Buenos Aires, Buenos Aires, Argentina
[3] Instituto Antártico Argentino, Instituto Nanobiotec, CONICET-Universidad de Buenos Aires, Buenos Aires, Argentina
Full list of author information is available at the end of the article

Donalle *et al. Natural Products and Bioprospecting*   (2022) 12:26

Page 2 of 10

Graphical Abstract
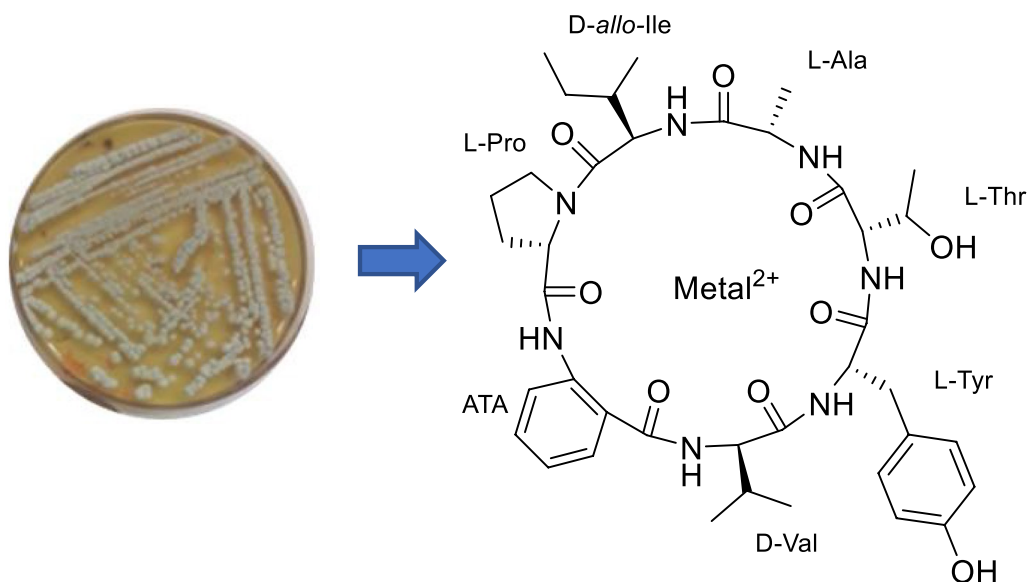
1 Introduction

Marine fungi are known to produce metabolites with a plethora of bioactivities, which include antimicrobial, antiviral, antitumoral, anti-inflammatory activities among others. Notably, marine natural products (MNP) from fungi represent nearly half of all reported MNP [1, 2]. Fungi isolated from Antarctic environments are not an exception and are also well-known as producers of bioactive metabolites [3, 4]. *Cadophora* is a worldwide ubiquitous genus with 43 species nowadays [5] some of which, including *C. malorum*, were reported from Antarctica locations [6]. Some *Cadophora* isolates have been reported to produce a series of bioactive metabolites with a wide range of structural scaffolds [7–9].

Metallomics integrates multidisciplinary research for the study of the relationships between bio-metals to bio-function. One of the fields of increasing interest in this area is the study of the metal coordination capability of metabolites, which may account for many biological activities such as metal hijacking, resistance to reactive oxygen species, production of sexual spores in microorganisms [10].

Electrospray ionization (ESI), a soft ionization technique able to transfer ions from solution to the gas phase, has been previously employed for the evaluation of the metal binding nature of secondary metabolites. Metal ions of alkali, alkaline earth and transition metals have been widely used in ESI, in order to record spectra of mixtures of metal salt solutions and samples, or by

post-HPLC column addition of metal salt solutions [11, 12]. In particular, the latter technique has been applied as a screening method for the detection of compounds with metal binding properties [12, 13].

As part of the search for new natural products produced from Antarctica-derived fungi, the LC–MS runs of extracts obtained from a collection of 26 strains were chemometrically analysed employing MS-DIAL [14] and an outlier sample, *C. malorum*, was selected. Two new cyclic peptides (cadophorins A and B) were isolated and identified from this extract. Since there are previous reports of cyclic peptides with metal binding properties [15], cadophorins A and B were evaluated as potential metal binders of alkaline-earth metals, Zinc and Copper. The new peptides showed the capability to form complexes with all the metals, although the stability of the formed species was higher in the case of Copper, Zinc and Magnesium. Although metal binding properties may account for certain bioactivities like ionophoric action [16], metal binders can be useful as well as self-assembling structures to construct ion channels in supramolecular chemistry, and also as asymmetric catalysts [17, 18].

2 Results and discussion

The organic extracts of small cultures of *C. malorum* and other 25 strains isolated from Antarctic soil samples were analysed by LCMS using Electrospray in positive and negative ion mode, and the runs were screened using the free platform MS-DIAL [14]. Principal component

analysis (PCA), applied to the negative ion mode data, showed in the score plot an outlier strain, *C. malorum.* (Additional file 1: Fig. S1). A search on the ion table for unique metabolites, which were present in only one PCA class (Additional file 1: Fig. S2), and the PCA loading plot, exposed the presence of two metabolites of peptidic nature, according to their MS2 spectra, with molecular weights of 763 and 777.

Based on this result, the components of the organic extract of *C. malorum* were separated by HPLC yielding two compounds, which were named cadophorins A and B (Fig. 1). Both compounds were considered pure after analysis by LCMS and ^{1}H NMR in CDCl$_3$/CD$_3$OD. However, some duplicated nonexchangeable signals were observed in the ^{1}H NMR spectra in DMSO-d_6 or CD$_3$OD (Additional file 1: Fig. S3.8). This fact indicated that the compounds exist in a slow conformational equilibrium in these solvents [19].

Cadophorin A (cadA) has a molecular formula of C$_{39}$H$_{54}$N$_7$O$_9$ as determined by HRESIMS. The MS/MS spectrum showed the presence of characteristic signals corresponding to the loss of some amino acids like alanine (Ala), threonine (Thr), tyrosine (Tyr), valine (Val) and leucine or isoleucine (Ile), although the structure could not be fully determined considering proteinogenic amino acids only. The ^{13}C NMR (Table 1) and HSQC-DEPT spectra exhibited 12 aromatic carbon signals accounting for two phenyl groups, seven carbonyl signals and five methylene, nine methine and six methyl group signals (Table 1). The 2D NMR data (COSY, HSQC and HMBC) established substructures matching with Ala, Thr, Tyr, Val, Ile, Pro and an anthranilic acid residue (ATA). This last fragment exhibited a characteristic

system of four consecutive aromatic protons (δ_H 8.48, br d, $J = 8.0$ Hz; δ_H 7.49, dt, $J = 8.0$, 1.3 Hz; δ_H 7.13, dt, $J = 8.0$, 1.0 Hz; δ_H 7.79, dd, $J = 8.0$, 1.3 Hz). The sequence of the amino acids was established by analyses of HMBC and NOESY correlations, in combination with Mass Spectrometry. An Ala was positioned between Thr and Ile by the HMBC correlations of Ala-NH (δ_H 7.42 ppm) to C-1 (δ_C 170.3) of Thr and of Ile-NH (δ_H 8.23 ppm) to C-1 of Ala (δ_C 172.0 ppm). In the same way, Thr was attached to a Tyr by the HMBC correlations of Thr-NH (δ_H 8.33 ppm) and Thr-H-2 (δ_H 4.05 ppm) to Tyr-C-1 (δ_C 171.9). At the same time, Tyr-NH (δ_H 8.18 ppm) correlated to Val-C-1 (δ_C 170.2). A NOESY correlation of Val-NH (δ_H 8.13 ppm) to ATA-H-3 (δ_H 7.79 ppm) allowed us to place Val next to ATA. Moreover, the connectivity between ATA and Pro was identified based on an HMBC correlation of ATA-NH (12.03 ppm) and Pro-C-1 (δ_C 170.6 ppm). Finally, a NOESY correlation between Pro-H-5 (δ_H 3.67–3.69 ppm) and Ile-H-2 (δ_H 1.85 ppm) connected Pro to Ile and closed the cycle. Other HMBC and NOESY correlations supported this planar structure (Fig. 2 and Additional file 1: Figs. S3.1–S3.7, S3.9–S3.11), as well as a detailed analysis of the MS/MS spectrum (Additional file 1: Table S3.1). The *trans* configuration of Pro can be deduced from the difference between δ_C C-3 and δ_C C-4 [15].

The absolute configuration of each amino acid was determined via Marfey's analysis. Cadophorin A was hydrolysed, and the hydrolysate was derivatized with *N*-(2,4-dinitro-5-fluorophenyl)-ʟ-valinamide (ʟ-FDVA, Marfey's reagent) followed by HPLC–DAD/MS analysis and comparison with authentic standards of Marfey's derivatized amino acid [20]. For the separation of
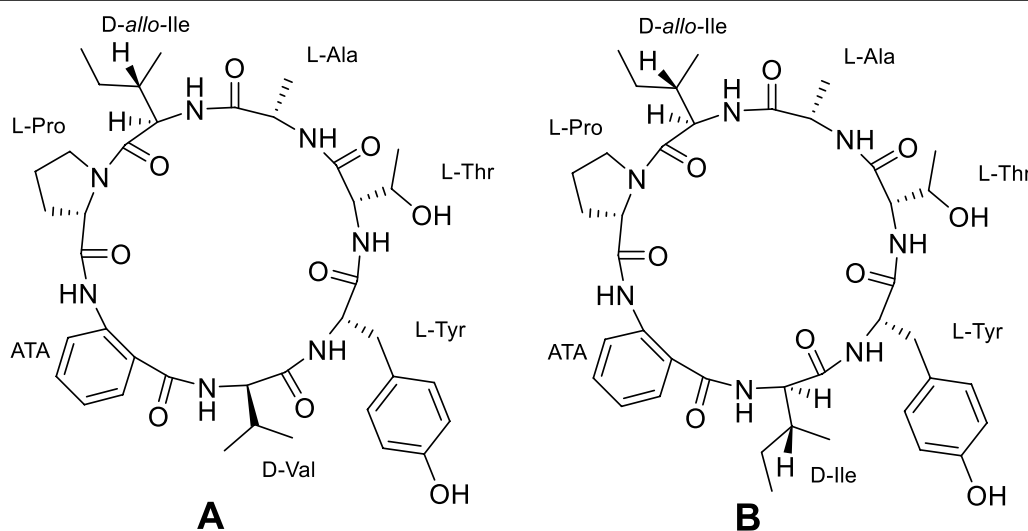

Fig. 1 Cadophorins A and B isolated from *Cadophora malorum*. **A** is cadophorin A and **B** is cadophorin B

Donalle *et al. Natural Products and Bioprospecting*   (2022) 12:26

Page 4 of 10

Table 1 ^{13}C NMR (500 MHz) and ^{1}H NMR (125 MHz) data for cadophorins A and B

	Number	Cadophorin A		Cadophorin B	
		δ_C, type	δ_H, (*J* (Hz))	δ_C, type	δ_H, (*J* (Hz))
L-Ala	NH		7.42, d (6.5)		7.42, d (6.5)
	1	172.0, CO		172.0, CO	
	2	49.2, CH	4.32, qi (6.5)	49.2, CH	4.32, qi (6.5)
	3	20.9, CH$_3$	1.32, d (6.5)	20.8, CH$_3$	1.32, d (6.5)
D-*allo*-Ile	NH		8.23, d (9.4)		8.22, d (9.5)
	1	170.7, CO		170.7, CO	
	2	52.3, CH	5.27, dd (9.4, 2.6)	52.3, CH	5.27, dd (9.5, 2.4)
	3	37.3, CH	1.85, m	37.3, CH	1.85, m
	4	27.0, CH$_2$	1.21, m	27.0, CH$_2$	1.21, m
	5	12.4, CH$_3$	1.03, t (7.1)	12.3, CH$_3$	1.03, t (7.2)
	6	15.1, CH$_3$	0.83, d (6.9)	15.1, CH$_3$	0.83, d (6.8)
L-Pro	1	170.6, CO		170.6, CO	
	2	62.2, CH	4.40, dd (8.6, 1.5)	62.2, CH	4.40, dd (8.7, 1.7)
	3	29.8, CH$_2$	2.12, 2.01, m	29.9, CH$_2$	2.12, 2.01, m
	4	24.1, CH$_2$	1.97, 1.76, m	24.1, CH$_2$	1.97, 1.75, m
	5	46.6, CH$_2$	3.71, 3.67 m	46.7, CH$_2$	3.72, 3.67, m
ATA	NH		12.03, s		11.99, s
	1	168.3, CO		168.3, CO	
	2	119.7, C		119.7, C	
	3	129.2, CH	7.79, dd (8.0, 1.3)	129.2, CH	7.76, dd (8.0, 1.3)
	4	123.0, CH	7.13, dt (8.0, 1.0)	123.0, CH	7.12, dt (8.0, 1.1)
	5	132.9, CH	7.49, dt (8.0, 1.3)	132.9, CH	7.48, dt (8.0, 1.1)
	6	119.3, CH	8.48, *br* d (8.0)	119.3, CH	8.48, d (8.0)
	7	139.5, C		139.5, C	
D-Val	NH		8.13, d (9.0)		
	1	170.2, CO			
	2	57.0, CH	4.78, dd (9.0, 4.0)		
	3	31.8, CH	2.08, m		
	4	19.9, CH$_3$	0.92, d (6.8)		
	5	17.0, CH$_3$	0.50, d (6.8)		
D-Ile	NH				8.15, d (8.9)
	1			170.2, CO	
	2			57.0, CH	4.77, dd (8.9, 4.4)
	3			38.4, CH	1.8, m
	4			23.7, CH$_2$	0.93, m
	5			12.0, CH$_3$	0.74, t (7.2)
	6			15.8, CH$_3$	0.86, d (6.7)
L-Tyr	NH		8.16, d (10.2)		8.16, d (10.1)
	1	171.9, CO		171.9, CO	
	2	56.8, CH	4.62, dt (10.2, 5.2)	56.8, CH	4.65, dt (10.1, 5.2)
	3	36.5, CH$_2$	2.96, 2.93, m$_{AB}$	36.5, CH$_2$	2.95, m
	4	128.1, C		128.0, C	
	5	130.3, CH	7.06, d (8.5)	130.3, CH	7.04, d (8.6)
	6	115.5, CH	6.66, d (8.5)	115.4, CH	6.66, d (8.6)
	7	156.4, C		156.4, C	
L-Thr	NH		8.33, d (9.6)		8.37, d (9.6)
	1	170.3, CO		170.3, CO	
	2	59.0, CH	4.05, dd (9.6, 2.4)	59.0, CH	4.06, dd (9.6, 2.3)

Table 1 (continued)

Number	Cadophorin A		Cadophorin B	
	δ_C, type	δ_H, (*J* (Hz))	δ_C, type	δ_H, (*J* (Hz))
3	66.8, CH	4.12, m	66.8, CH	4.12, m
4	21.2, CH$_3$	1.02, d (6.0)	21.2, CH$_3$	1.02, d (6.1)
OH		5.15, d (4.3)		5.18, s

the diasteromeric D-*allo*-Ile and D-Ile MR derivatives, a PFP HPLC column was employed [21]. This experiment revealed the presence of L-Ala, L-Thr, L-Tyr, D-Val, L-Pro and D-*allo*-Ile in cadophorin A (Table 2). The presence of D-*allo*-Ile was confirmed by co-injection of the L-FDVA derivative of D-*allo*-Ile and cadophorin A. Although PFP phase has been used previously for this application [21], in this work a different set of chromatographic conditions allowed a better differentiation of the four stereoisomers

of isoleucine. Temperature is also an important factor for this separation, and higher temperatures were counterproductive in this respect.

Cadophorin B (cadB) showed a signal m/z 778.4135 corresponding to a protonated molecule with a molecular formula $C_{40}H_{55}N_7O_9$ in the ESI-HR spectrum. The NMR spectra of cadophorin B were very similar to those of cadophorin A. The main difference was the absence of the methyl signals of D-Val and the appearance of the

Fig. 2 Relevant correlations observed in 2D NMR experiments. **A** is cadophorin A and **B** is cadophorin B
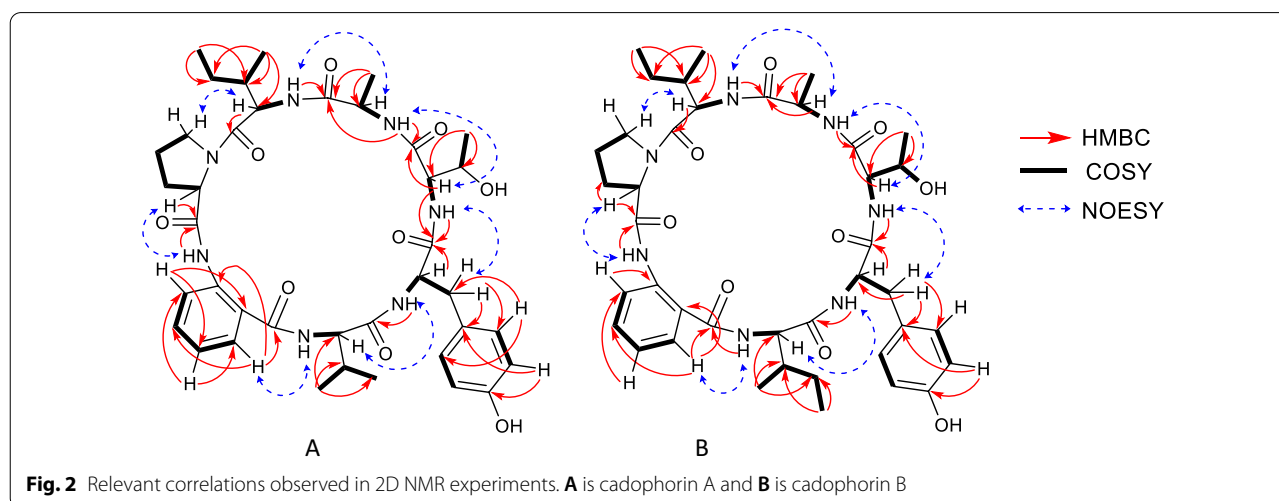
Table 2 Table retention times (R_T) of amino acid L-FDVA derivatives

Amino acid	Theoretical m/z [M+H]$^+$	Molecular formula [M+H]$^+$	Standard amino acid		Cadophorin A			Cadophorin B		
			Serie L	Serie D	m/z	$T_{R(min)}$	Error (ppm)	m/z	$T_{R(min)}$	Error (ppm)
			$T_{R(min)}$	$T_{R(min)}$						
Ala	370.1357	$C_{14}H_{19}N_5O_7$	13.3	16.5	370.1349	13.4	2.3	370.1343	13.5	3.9
Pro	396.1513	$C_{16}H_{21}N_5O_7$	12.6	15.1	396.1532	12.6	4.5	396.1505	12.6	2.3
allo-Ile	412.1826	$C_{17}H_{25}N_5O_7$	19.2	23.4	412.1807	23.5	4.7	412.1810	23.4	4.1
Ile	412.1826	$C_{17}H_{25}N_5O_7$	19.4	23.6	–	–	–	412.1825	23.6	0.5
Thr	400.1462	$C_{15}H_{21}N_5O_8$	8.4	12.9	400.1474	8.4	2.9	400.1466	8.4	0.9
Tyr*	742.2427	$C_{31}H_{35}N_9O_{13}$	29.5	32.7	742.2408	29.5	2.5	742.2430	29.5	0.5
Val	398.1670	$C_{16}H_{23}N_5O_7$	17.0	21.5	398.1647	21.0	6.0	–	–	–

* Disubstituted derivative

signals of two methyl groups at δ_H 0.86 (d) and 0.74 (t) in the ^{1}H NMR spectrum (Table 1), inferring the presence of an Ile instead of Val. 2D NMR spectra and MS and MS2 data confirmed this assumption (Additional file 1: Figs S4.1–S4.12) and all the correlations in the HMBC and NOESY spectra also corroborated the similarity between cadA and cadB (Fig. 2). Cadophorin B was hydrolised and derivatised in the same way as cadA and the analysis of the L-FDVA derivatised amino acids revealed a similar absolute configuration of the amino acids as in cadA and the presence of an additional D-Ile. Co-injection with authentic samples of derivatised D-Ile and D-*allo*-Ile showed that both aminoacids were present (Additional file 1: Fig. S5). Considering the similarity of cadophorin A and B, and the way this kind of peptides are biosynthesed [22], it can be assumed that D-Ile is in the same position as D-Val in cadophorin A.

The presence of D-*allo*-Ile in cyclic peptides produced by microorganisms is quite common, however this is not the case for D-Ile. The monamycins, which are antibiotic hexapeptides are probably the only example of natural cyclic peptides incorporating this amino acid [23]. D-Ile has an opposite configuration at C-3 compared to L-Ile or D-*allo*-Ile. Since this position is not vicinal to the carboxyl group of the aminoacid, D-Ile cannot be biosynthetised by the typical enolisation/epimerization sequence. Instead, biosynthetic studies have shown that the epimerization at C-3 occurs through an α-keto acid intermediate [24]. Since the report of the monamycins, other cyclic peptides containing this amino acid were informed, although their structures were not adequately confirmed or were incorrect [25, 26].

The cyclization of a linear peptide normally contributes to substantial conformational rigidity over the linear form, which explains the specificity of cyclic peptides for target sites and their increased resistance towards proteases. Proline itself gives a strong conformational rigidity compared to other amino acids, but the presence of ATA attached to Pro in a cyclic peptide further restricts the flexibility of the molecules. 3D structures of the lower energy conformers of cad1 are shown in Additional file 1: Fig. S7.1.

There are a few examples of cyclic peptides with this sequence ATA-Pro or p-hydroxy ATA-Pro, like the tricyclic peptide psychrophilin A, isolated from the psychrotolerant fungus *Penicillium ribeum* [27] and asperpetide A from a gorgonian-derived *Aspergillus* sp. [28].

Cadophorins were analysed by LCMS with post-column *in source* addition of metal chloride solutions of Magnesium, Calcium, Strontium, Copper, and Zinc to test their metal binding properties. These metals, except for Strontium, were selected due to their metabolic importance in living organisms, while Strontium was included in order to compare its performance with the other alkaline earth metals. The mass spectra showed the presence of a signal corresponding to the ion $[cad + Me]^{2+}$, where Me is any metal, in all the cases as the main signal (Additional file 1: Fig. S6.1). The response of that signal was plotted for cadB giving a descending order of response from Sr, Ca, Mg, Zn to Cu (Additional file 1: Fig. S6.2). This response is related to the ease of ionization. When comparing related compounds, the less polar and less solvated species are nearest to the surface of the electrosprayed droplet and are easily ionised. In this sense, the relationship between the responses of alkaline earth complexes could be predicted (Sr > Ca > Mg). These MS experiments are also strongly influenced by the kinetics, as the complexes are formed in situ without time for equilibration, and for this reason the comparison between Mg, Cu and Zn complexes is not straightforward and would require additional kinetic studies.

The optimised structures of the complexes of cadA with different metals were calculated by DFT methods to correlate the MS results with the stability of the complexes, which are shown in Fig. 3. The site of coordination to the divalent cation was the oxygen of carbonyl moieties in all the cases. The geometry observed around the metal center was trigonal bipyramidal for Mg, Cu and Zn, with carbonyls of ATA, Val, Thr in equatorial and Pro and Tyr in the axial positions. In the case of Ca and Sr, an additional coordination to the carbonyl of the *allo*-Ile resulted in a distorted octahedral geometry. The relevant interatomic distances for the metal complexes are shown in Additional file 1: Table S7.1. These geometries and the distances from the cation to the carbonyl oxygen are typical for these metal cations [29].

For most of the complexes $[cadA + Me]^{2+}$ (Me = Mg, Ca, Sr, Zn), an additional isomer of higher energy was found, also with trigonal bipyramidal geometry, which coordinates the divalent cation with the carbonyls of Pro, Ser and Val equatorially and Tyr and *allo*-Ile in the axial positions. This additional mode of coordination holds the metal in a central position, which is less exposed to the surface of the molecule (Additional file 1: Table S7.2).

The calculated energies for the lower energy conformers are shown in Table 3, and show an order of stabilities: Cu > Zn > Mg > Ca > Sr. These results indicate that the metal complexes of cadophorins are more stable in the case of the smaller metal cations Cu, Zn and Mg which have similar ionic radii.

It is worth to mention that the employed MS methodology allowed the evaluation of the binding properties of cyclic peptides present in small amounts, with the advantage of allowing hundreds of experiments using the same sample.
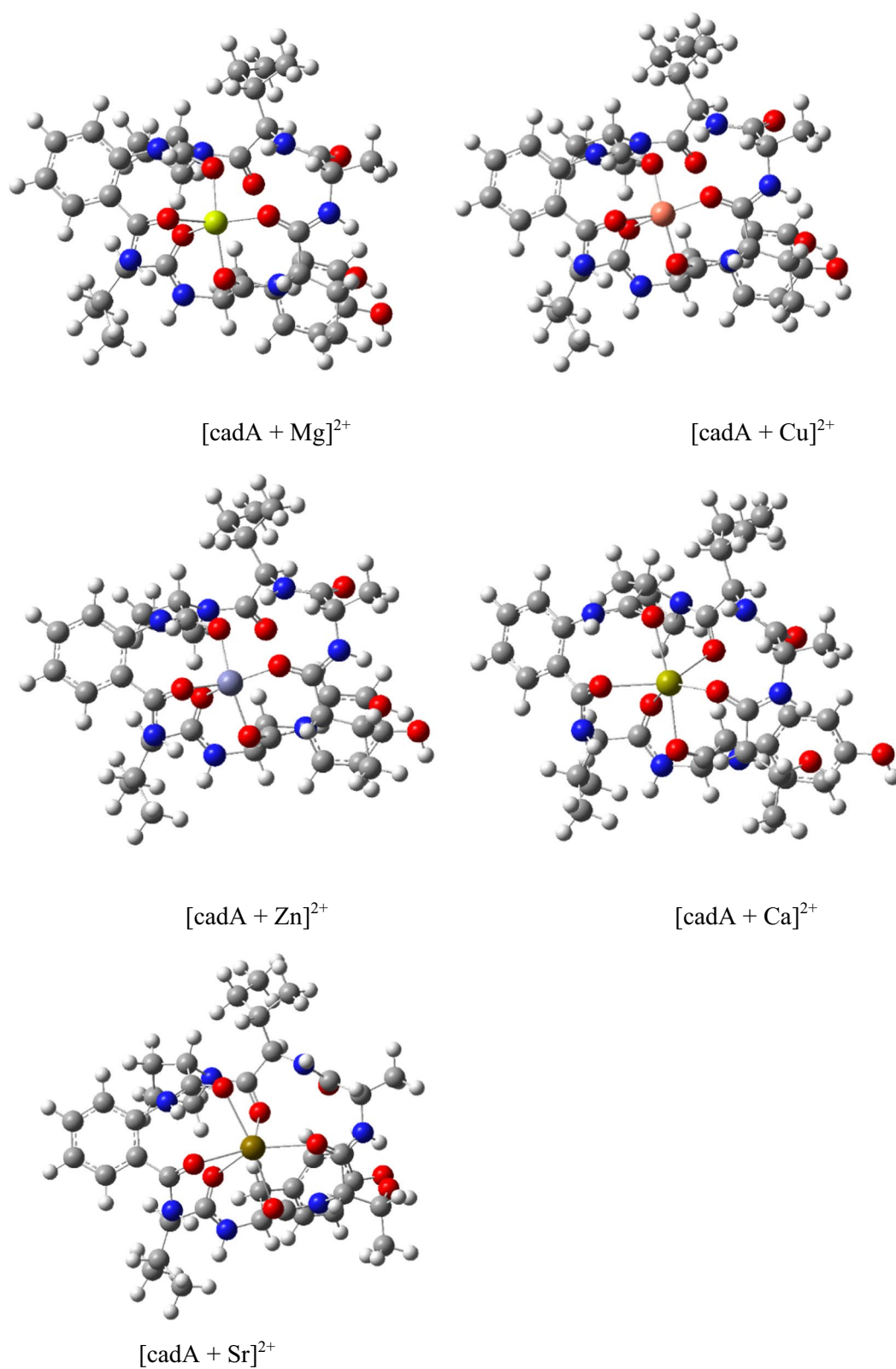
[cadA + Mg]²⁺

[cadA + Cu]²⁺

[cadA + Zn]²⁺

[cadA + Ca]²⁺

[cadA + Sr]²⁺

Fig. 3 Optimised structures of cadA–Me complexes calculated at the B3LYP level of theory, Me = Mg^{2+} and Cu^{2+}

Donalle *et al. Natural Products and Bioprospecting*   (2022) 12:26

Page 8 of 10

Table 3 Optimised energies for cadA–Me complexes $[cadA + Me]^{2+}$ calculated at the B3LYP level of theory, $Me = Mg^{2+}, Ca^{2+}, Sr^{2+}, Zn^{2+}$ and Cu^{2+} for: $cadA + Me(H_2O)_6^{2+} \rightarrow [cadA + Me]^{2+} + 6 H_2O$

Me	Base	$\Delta G°$ (kcal/mol)	$\Delta H°$ (kcal/mol)
Mg	6-31G(d)	− 40.21	− 1.17
Ca	6-31G(d)	− 37.78	− 2.76
Sr	LANL2DZ	− 20.38	14.51
Sr	6-31G(d)/LANL2DZ	− 8.05	24.84
Zn	6-31G(d)	− 47.72	− 12.15
Cu	6-31G(d)	− 59.51	− 20.60

Cadophorins A and B showed antifungal activity against *Candida albicans* and *C. haemulonii* at 20 μg/spot (Additional file 1). The extract of *C. malorum* possessed also antifungal activity against phytopathogenic strains, which was attributed to the presence of wortmannin, a known antifungal metabolite, also present in the extract (Additional file 1: Fig. S8) [30].

3 Experimental section

3.1 General experimental procedures
Optical rotations were recorded on a PerkinElmer 343 polarimeter. Electronic Circular Dichroism spectra were determined in a Jasco J815 Spectropolarimeter. ^{1}H- and ^{13}C-NMR spectra were obtained on a Bruker Avance Neo 500 spectrometer operating at 500 MHz and 125 MHz, respectively; chemical shifts (δ_H and δ_C) are informed in ppm, *J* in Hz. Two-dimensional NMR spectra (COSY, HSQC-DEPT, NOESY and HMBC) were recorded using standard Bruker software. HR (ESI) mass spectra and HPLC–MS runs were recorded using a MicrOTOF QII Bruker mass spectrometer. All solvents were distilled before use. LC/MS-grade methanol and water were purchased from Carlo Erba (Milan, Italy). Formic acid (p.a., ACS) was purchased from Merck (Merck KGaA, Darmstadt, Germany). Standard amino acids were purchased from Sigma-Aldrich (Merck KGaA, Darmstadt, Germany), except for D-Isoleucine which was purchased from TCI (Tokyo Chemical Industry Co., Ltd, Alpharetta, USA).

3.2 Isolation and cultivation of Antarctic fungi
Soil samples were collected at Potter Peninsula, 25 de Mayo/King George Island (62° 14′ 18″ S, 58° 40′ 00″ W) Antarctica by M.M.M. and L.R.. For experimental details, see Additional file 1. The strain of *C. malorum* was classified by M.M.M. and L.R., deposited in the Culture Collection at the Argentinean Antarctic Institute (IAA) and the DNA sequences were submitted to GenBank under Accession Number OM177061.

3.3 Cultivation of *Cadophora malorum*
For the large-scale cultures used for compound isolation, *Cadophora malorum* was grown on PDA for at 15 °C for 14 days. From these plates, small plugs of the culture were transferred into Erlenmeyer flasks containing Potato Dextrose Broth (PDB) and incubated at 15 °C and 200 rpm for 4 weeks. Supernatant was separated from the biomass by centrifugation at 4000 rpm for 10 min.

3.4 Extraction and isolation of the metabolites.
The supernatant (1.5 L) was extracted with ethyl acetate (3 × 500 mL) and the organic extract (100 mg) was subjected to HPLC (column: YMC C18, 5 μm, 22.5 × 2.5 cm; MeOH-H$_2$O 55:45) yielding cadophorin B (1.8 mg), cadophorin A, re-purified by the same technique (1.0 mg), and a fraction which was separated by prep. TLC (MeOH:CH$_2$Cl$_2$ 5:95) yielding 2.4 mg of wortmannin.

3.5 Marfey's derivatives
A sample of cadA and cadB (approximately 0.5 mg) were dissolved in 2.0 mL of 6 M hydrochloric acid and hydrolyzed overnight at 110 °C. The hydrolysates were treated with Marfey's reagent (FDNP-Val-NH$_2$) as previously reported [31]. The derivatives were analysed by LC–DAD–MS (column: Luna PFP, 3 μm, 2.0 mm × 100 mm; Phenomenex, Torrance, CA, USA), set at 28 °C. The mobile phase was H$_2$O containing 0.1% formic acid (A) and ACN (B), at a flow rate of 0.3 mL/min. A linear gradient elution was performed as follows: 25% B (3 min), 25–65% B (3–40 min), 100% B (41–45 min), 25% B (45–50 min).

The same procedure was repeated for cadophorin B (0.2 mg) to confirm the results.

3.6 Binding metal experiments
The MS instrument with an ESI source was operated using the following conditions: capillary voltage 4.5 kV; end plate offset 500 V; dry temperature 200 °C. Nitrogen was used as dry gas (11.0 L/min) and as nebuliser gas (nebuliser pressure 3.4 bar). Data acquisition and processing were performed using Bruker Compass Data Analysis software. A Luna PFP HPLC column (3 μm, 2.0 mm × 100 mm; Phenomenex, Torrance, CA, USA), set at 30 °C, was employed as the stationary phase. The mobile phase was water containing 0.1% formic acid (A) and MeOH (B), at a flow rate of 0.3 mL/min. Linear gradient elution was performed as follows: 55% B (0–2 min), 55–100% B (2–7 min), 100% B (7–14 min).

Post-column addition of metal solutions. An aqueous solution (10 mM) of MgCl$_2$, CaCl$_2$, SrCl$_2$, CuCl$_2$ or ZnCl$_2$ was introduced using a syringe pump at a flow rate of 3 μL/min, via a T-junction before entrance into the ion

Donalle *et al. Natural Products and Bioprospecting*   (2022) 12:26

Page 9 of 10

source. The solutions of metals were previously titrated with an EDTA solution employing murexide (Ca^{2+} and Cu^{2+}) or Eriochrome Black T (Mg^{2+}, Zn^{2+}) as indicators.

3.7 Antifungal assays
For experimental details, see Additional file 1.

3.8 Computational section
See Additional file 1.

3.9 Compound information
Cadophorin A. White amorphous solid; $[\alpha]_D^{20}$ − 11.8 (*c* 0.065, CHCl$_3$). UV (MeOH) λ_{max} (log ε) 271 (3.0), 245 (3.3) nm. ^{1}H NMR and ^{13}C NMR (see Table 1). Positive ion HRESIMS m/z 764.3983 (Calcd for $C_{39}H_{54}N_7O_9$ [M+H]$^+$, 764.3978).

Cadophorin B. White amorphous solid; $[\alpha]_D^{20}$ − 35.1 (*c* 0.080, CHCl$_3$). UV (MeOH) λ_{max} (log ε) 271 (3.0), 245 (3.4) nm. ^{1}H NMR and ^{13}C NMR (see Table 1). Positive ion HRESIMS m/z 778.4134 (Calcd for $C_{40}H_{56}N_7O_9$ [M+H]$^+$, 778.4108).

Supplementary Information
The online version contains supplementary material available at https://doi.org/10.1007/s13659-022-00348-x.

Additional file 1. PCA analysis (score plot); Spectroscopical data (^{1}H NMR, ^{13}C NMR, ^{1}H,^{1}H COSY, HSQC, HMBC, NOESY, HRMS (ESI), MS/MS spectra, ECD) of cadophorins A and B; Comparison of the retention times of the L-FDVA derivatives of D-Ile, D-*allo*-Ile present in cadophorin B, to co-injected standards; MS spectra of cadophorin B with post-column *in source* addition of metal salt solutions; Optimized structures and geometrical parameters of metal complexes calculated at the B3LYP level of theory; ^{1}H NMR and ^{13}C NMR of wortmannin; Isolation and cultivation of Antarctic fungal strains; Antifungal assay.

Author contributions
GD: isolation, structural elucidation, spectrum analysis. MMM: isolation and identification of strains, antifungal assay. GES.: molecular modelling. LR: supervision (microbiology), funding acquisition. GMC: MS experiments, supervision (chemistry), funding acquisition, writing. All authors read and approved the final manuscript.

Declarations

Competing interests
No conflict of interest is declared.

Author details
^{1}Facultad de Ciencias Exactas y Naturales, Departamento de Química Orgánica, Universidad de Buenos Aires, Buenos Aires, Argentina. ^{2}Unidad de Microanálisis y Métodos Físicos Aplicados a la Química Orgánica (UMYMFOR), CONICET-Universidad de Buenos Aires, Buenos Aires, Argentina. ^{3}Instituto Antártico Argentino, Instituto Nanobiotec, CONICET-Universidad de Buenos Aires, Buenos Aires, Argentina.

References
1. Yurchenko AN, Girich EV, Yurchenko EA. Metabolites of marine sediment-derived fungi: actual trends of biological activity studies. Mar Drugs. 2021;19:88.
2. Carroll AR, Copp BR, Davis RA, Keyzers RA, Prinsep MR. Marine natural products. Nat Prod Rep. 2021;38:362–413.
3. Shi T, Yu YY, Dai JJ, Zhang YT, Hu WP, Zheng L, Shi DY. New polyketides from the antarctic fungus *Pseudogymnoascus* sp. HSX2#-11. Mar Drugs. 2021;19:168.
4. Vaca I, Chávez R. Bioactive compounds produced by Antarctic filamentous fungi. In: Rosa LH, editor. Fungi of Antarctica. Diversity, ecology and biotechnological applications. Heidelberg: Springer; 2019. p. 265–83.
5. Index Fungorum. http://www.indexfungorum.org/.
6. Iliushin VA. First find of *Cadophora antarctica* Rodr.-Andrade, Stchigel, Mac Cormack & Cano in the Arctic. Czech Polar Rep. 2020;10:147–52.
7. Rusman Y, Held BW, Blanchette RA, Wittlin S, Salomon CE. Soudanones A-G: Antifungal isochromanones from the ascomycetous fungus *Cadophora* sp. isolated from an iron mine. J Nat Prod. 2015;78:1456–60.
8. Almeida C, Eguereva E, Kehraus S, Siering C, König GM. Hydroxylated sclerosporin derivatives from the marine-derived fungus *Cadophora malorum*. J Nat Prod. 2010;73:476–8.
9. Rusman Y, Held BW, Blanchette RA, He Y, Salomon CE. Cadopherone and colomitide polyketides from *Cadophora* wood-rot fungi associated with historic expedition huts in Antarctica. Phytochem. 2018;148:1–10.
10. Patil RH, Luptáková D, Havlíček V. Infection metallomics for critical care in the post-COVID era. Mass Spectrom Rev. 2021. https://doi.org/10.1002/mas.21755.
11. Butler M, Cabrera GM. A mass spectrometry-based method for differentiation of positional isomers of monosubstituted pyrazine N-oxides using metal ion complexes. J Mass Spectrom. 2015;50:136–44.
12. Cirigliano AM, Rodriguez MA, Gagliano ML, Bertinetti BV, Godeas AM, Cabrera GM. Liquid chromatography coupled to different atmospheric pressure ionization sources-quadrupole-time-of-flight mass spectrometry and post-column addition of metal salt solutions as a powerful tool for the metabolic profiling of *Fusarium oxysporum*. J Chromatogr A. 2016;1439:97–111.
13. Kempen EC, Brodbelt JS. Screening metal binding selectivities of macrocycle mixtures by HPLC-ESI-MS and post-column reactions. Anal Chem. 2001;73:384–90.
14. Tsugawa H, Cajka T, Kind T, Ma Y, Higgins B, Ikeda K, Kanazawa M, Vander GJ, Fiehn O, Arita M. MS-DIAL: data independent MS/MS deconvolution for comprehensive metabolome analysis. Nat Methods. 2015;12:523–6.
15. Lawrence RG, Rodney MC. Metal complexes of synthetic cyclic peptides. Polyhedron. 2018;153:1–23.
16. Chermahini AN, Chermahini ZJ. Comparing the ion affinity of two ionophores: theoretical study of alkali earth metal ion–nano tubular cyclic peptide complexes. J Mol Liq. 2016;214:101–10.
17. Song Q, Cheng Z, Kariuki M, Hall SCL, Hill SK, Rho JY, Perrier S. Molecular self-assembly and supramolecular chemistry of cyclic peptides. Chem Rev. 2021;121:13936–95.
18. Zheng L, Marcozzi A, Gerasimov JY, Herrmann A. Conformationally constrained cyclic peptides: powerful scaffolds for asymmetric catalysis. Angew Chem Int Ed. 2014;53:7599–603.
19. Tabudravu JN, Jaspars M, Morris LA, Kettenes-van den Bosch JJ, Smith N. Two distinct conformers of the cyclic heptapeptide phakellistatin 2 isolated from the Fijian marine sponge *Stylotella aurantium*. J Org Chem. 2002;67:8593–601.
20. Bhushan R, Brückner H. Marfey's reagent for chiral amino acid analysis: a review. Amino Acids. 2004;27:231–47.
21. Zhou T, Katsuragawa M, Xing T, Fukaya K, Okuda T, Tokiwa T, Tashiro E, Imoto M, Oku N, Urabe D, Igarashi Y. Cyclopeptides from the mushroom pathogen fungus *Cladobotryum varium*. J Nat Prod. 2021;84:327–38.
22. Finking R, Marahiel MA. Biosynthesis of nonribosomal peptides. Annu Rev Microbiol. 2004;58:453–88.

23. Bevan K, Davies JS, Hassall CH, Phillips DAS. D-Isoleucine, an exceptional amino-acid residue of the antibiotic monamycin. J Chem Soc Chem Commun. 1969;21:1246.
24. Davies JS, Foley MH, Hassall CH, Arroyo V. The biosynthetic origin of D-Isoleucine in the monamycins. J Chem Soc Chem Commun. 1973;20:782–3.
25. Matsuda K, Kuranaga T, Sano A, Ninomiya A, Takada K, Wakimoto T. The revised structure of the cyclic octapeptide surugamide A. Chem Pharm Bull. 2019;67:476–80.
26. Wen W, Huanqin D, Li B, Biao R, Jingcai L, Yuanming L, Liangdong G, Lixin Z, Hongwei L. Isolation and structural elucidation of proline-containing cyclopentapeptides from an endolichenic *Xylaria* sp. J Nat Prod. 2011;74:1303–8.
27. Dalsgaard PW, Ostenfeld TL, Frydenvang K, Christophersen C. Psychrophilin A and cycloaspeptide D, novel cyclic peptides from the psychrotolerant fungus *Penicillium ribeum*. J Nat Prod. 2004;67:878–81.
28. Min C, Chang-Lun S, Xiu-Mei F, Chui-Jian K, Zhi-Gang S, Chang-Yun W. Lumazine peptides penilumamides B—D and the cyclic pentapeptide asperpeptide A from a gorgonian-derived *Aspergillus* sp. fungus. J Nat Prod. 2014;77:1601–6.
29. Zheng H, Cooper DR, Porebski PJ, Shabalin IG, Handing KB, Minor W. CheckMyMetal: a macromolecular metal-binding validation tool. Acta Cryst. 2017;D73:223–33.
30. Dischler NM, Xu L, Li Y, Nichols CB, Alspaugh JA, Bills GF, Gloer JB. Wortmannin and wortmannine analogues from an undescribed *Niesslia* sp. J Nat Prod. 2019;82:532–8.
31. Ratnayake R, Fremlin LJ, Lacey E, Gill JH, Capon RJ. Acremolides A-D, Lipodepsipeptides from an Australian marine-derived fungus *Acremonium* sp. J Nat Prod. 2008;71:403–8.

Publisher's Note